FLUIDS IN THE DEEP EARTH: ESTIMATION OF FLUID FUGACITIES IN PERIDOTITES FROM THE KLAMATH MOUNTAINS, CALIFORNIA, USA

A Thesis

by

RYAN MICHAEL KISSINGER

Submitted to the Office of Graduate and Professional Studies of
Texas A&M University
in partial fulfillment of the requirements for the degree of

MASTER OF SCIENCE

Chair of Committee,	William Lamb
Co-Chair of Committee,	Julie Newman
Committee Member,	Franco Marcantonio
Head of Department,	Michael Pope

December 2018

Major Subject: Geology

ABSTRACT

Granulites-facies mineral assemblages typically require values of activity of H_2O (aH_2O) significantly less than unity, and these values are reduced relative to lower grade rocks. Possible mechanisms for lowering values of aH_2O during granulite facies metamorphism include partial melting or infiltration of a low aH_2O fluid. For example, it has been argued that the infiltration of a large amount of CO_2 could lower the aH_2O of rocks in the lower crust, and stabilize granulite-facies mineral assemblages. A third mechanism that could explain low values of aH_2O is the metamorphism of already dry rock.

The goal of this study is to evaluate granulite-forming mechanisms using peridotites from the Seiad Complex, Klamath Mountains, California. To accomplish this, we examined the nature of deep-seated fluids through the application of mineral equilibria, which are equations we used to quantify values of aH_2O and oxygen fugacity (fO_2). A dehydration reaction involving amphibole, for example, yields values of aH_2O ranging from 0.3 to 0.5, and spinel equilibria yield estimates of fO_2 that range from -2 to 0 log units relative to the FMQ buffer. Calculation of fluid speciation in the C-O-H system indicates that values of fO_2 recorded by some samples are inconsistent with a CO_2 or CH_4-rich fluid. Furthermore, the presence of an H_2O-rich fluid is inconsistent with values of aH_2O estimated using amphibole equilibria in these same rocks, which indicates there is no lithostatically pressured free fluid phase.

Clearly, the presence of amphibole in peridotites does not necessitate the presence of a H_2O-rich free fluid phase, nor oxidizing values of fO_2. The low values of aH_2O recorded by these rocks (< 0.5) are typical of granulite-facies metamorphism. If these rocks equilibrated at values of aH_2O that were less than 1 while in the mantle, similar to other mantle peridotites, then

low values of aH_2O recorded during subsequent granulite-facies metamorphism are likely a result of the recrystallization of already dry rock rather than infiltration of externally derived fluids with low aH_2O or partial melting.

CONTRIBUTORS AND FUNDING SOURCES

Contributors

This work was supported by a thesis committee consisting of Professors William Lamb and Julie Newman of the Department of Geology and Geophysics and Professor Franco Marcantonio of the Department of Oceanography.

All other work for the thesis was conducted by the student under the advisement of Professor William Lamb of the Department of Geology and Geophysics.

Funding Sources

Graduate study was supported by fellowships from Texas A&M University and the Houston Geological Society, and a research grant from the National Science Foundation.

TABLE OF CONTENTS

Page

LIST OF FIGURES

LIST OF TABLES

TABLE Page

INTRODUCTION

Values of activity of H_2O (aH_2O) in granulites are reduced relative to lower grade rocks, and typically range from 0.01 to 0.06 (Powell, 1983; Valley et al., 1983; Powers and Bohlen, 1985; Lamb and Valley, 1985; Lamb and Valley, 1988; Edwards and Essene, 1988). The early recognition of these relatively low H_2O activities was one of the motivating factors behind the investigation of various mechanisms that have been invoked to explain the stabilization of granulite-facies mineral assemblages (e.g., magmatic processes vs. the infiltration of low aH_2O fluids).

Partial melting may be an important process in high grade portions of the crust, and has long been considered a viable mechanism to account for the stabilization of granulite-facies mineral assemblages (Fyfe, 1973; Lamb and Valley, 1988). In this case, H_2O is partitioned preferentially into the melt, and if this melt rises in the crust, the refractory residuum will consist of dehydrated rocks metamorphosed to granulite-facies conditions (Fyfe, 1973; Valley et al., 1990; Valley, 1992).

Another granulite forming mechanism is the infiltration of fluids with inherently low H_2O activities. In these cases, the infiltration of fluids is thought to drive granulite-forming reactions and, therefore, the infiltrating fluid must be present in sufficient quantities to dilute fluids being produced by the break-down of hydrous minerals such as biotite or amphibole. It has been proposed, for example, that the formation of granulite-facies mineral assemblages in crustal rocks is driven by the infiltration of externally derived CO_2 (Newton et al., 1980; Janardhan et al., 1982; Condie et al., 1982; Friend, 1985; Newton, 1989; Santosh and Omori, 2008a). Lamb and Valley (1984) demonstrated that a CO_2 to rock ratio of approximately 0.1 would be required to form 10% orthopyroxene from the breakdown of amphibole. Thus, considerable volumes of

fluid may be required to stabilize granulite facies mineral assemblages on a terrane-wide basis. More recently, it has been suggested that the infiltration of brines, or a mixture of brines and CO_2 (likely immiscible) is responsible for generating the low values of aH_2O in granulites (Touret and Huizenga, 2012; Aranovich et al., 2014; Manning and Aranovich, 2014; Manning, 2018). These brines, if sufficiently saline, may have low values of aH_2O (Aranovich and Newton, 1996, 1997), and would likely be able to infiltrate low permeability silicate rocks (Watson and Brenan, 1987).

A third factor that could account for the low values of aH_2O recorded in rocks from the granulite-facies is the metamorphism (recrystallization) of rocks that were dry prior to granulite-facies metamorphism. For example, certain meta-igneous rocks may crystallize under H_2O undersaturated conditions. These rocks would not require any mechanism, such as partial melting or fluid infiltration, to generate low values of aH_2O, as removal or dilution of H_2O is not required (Valley, 1985; Valley et al., 1990).

Fluids also play an important role in mantle processes, and there are similarities between the nature of fluids, and the debate surrounding the nature of fluids, in the deep crust (granulite facies) and upper mantle. For example, H_2O affects temperatures and pressures of melting, and influences silicate melt compositions in mantle peridotites (Nicholls and Ringwood, 1972; Nicholls and Ringwood, 1973; Gaetani and Grove, 1998; Grove et al., 2012), and in crustal rocks (Clemens and Watkins, 2001; Clemens, 2006). Because H_2O behaves as an incompatible element during melting of mantle peridotites (Novella et al., 2014; Rosenthal et al., 2015), it will be incorporated into basaltic melts during melting at the mid-ocean ridge (Hirth and Kohlstedt, 1996). One consequence of this dehydration may be the generation of relatively anhydrous rocks (restites). Thus, the viscous discontinuity which exists at the boundary between the oceanic lithosphere and asthenosphere may be due to low H_2O contents of the lithospheric mantle that

are a result of partial melting (Hirth and Kohlstedt, 1996). In this case, melting of upwelling mantle produces a dehydrated restite (the lithosphere) just as melting in the lower crust may produce a dehydrated restite (granulites). Furthermore, it has been argued that grain boundary fluids are common in the upper mantle and that these fluids are comprised of CO_2 and brines (Andersen et al., 1984; Frezzotti and Touret, 2014), which is similar to the arguments made for rocks from the granulite facies (see above). Other studies have used equilibria among fluid species composed of C, O, and/or H (e.g., CO_2, H_2O, and CH_4) to evaluate if a lithostatically pressured fluid phase was present in the mantle (Lamb and Popp, 2009; Kang et al., 2017). Kang et al. (2017), for example, combined values of aH_2O and oxygen fugacity (fO_2) estimated for the same sample, and argued absence of a lithostatically-pressured fluid phase (e.g., grain boundaries fluids) in certain mantle rocks. Although low aH_2O fluids have been argued to play a role in stabilizing granulite-facies mineral assemblages by driving granulite forming reactions (Newton et al., 1980), this argument has not, to our knowledge, been applied to rocks from the mantle. Instead, models that invoke infiltration of low aH_2O fluids view the mantle as the ultimate source of these fluids (Santosh and Omori, 2008b; Touret and Huizenga, 2012).

Mineral equilibria are useful tools for investigating the nature of fluids in metamorphic rocks, and this approach has been applied to estimate values of fO_2 and aH_2O in rocks from the granulite-facies. In some cases, values of fO_2 are sufficiently reducing to rule out the presence of a CO_2-rich fluid (Lamb and Valley, 1985). Furthermore, when values of fO_2 and aH_2O have been determined for the same rock, it was demonstrated that certain rocks from the granulite-facies were metamorphosed in the absence of a lithostatically-pressured fluid, assuming no significant quantity of non-C-O-H fluid species was present (Lamb and Valley, 1984, 1985;

Edwards and Essene, 1988), which is a result consistent with other evidence for fluid absence (Clemens and Watkins, 2001).

We applied mineral equilibria to investigate the nature of fluids in orogenic peridotites from the Seiad complex. These samples originated in the mantle, and were emplaced in the crust where they experienced granulite-facies pressures (P) and temperatures (T). Estimation of values of aH_2O using dehydration equilibria involving amphibole, based on an approach similar to that of Lamb and Popp (2009), permits comparison with values from other granulite-facies rocks and mantle peridotites. Mineral equilibria are also used to determine values of oxygen fugacity, which, in some cases, places important constraints on the amount of CO_2 or CH_4 that is present. Finally, estimation of both fO_2 and aH_2O from the sample provides insight into the presence or absence of a grain-boundary C-O-H fluid.

GEOLOGIC SETTING

Samples were collected from the Klamath Mountains northwest California (Fig. 1). The Klamath Mountains are situated in the forearc of the modern-day Cascadia subduction zone along the border between northwest California and southwest Oregon. These mountains are thought to exemplify successive lateral accretion along a convergent margin (Wright and Fahan, 1988; Miller and Saleeby, 1991), and included in the Klamath Mountains is the Rattlesnake creek terrane (Wright and Wyld, 1994). Garlick et al. (2009) described the Rattlesnake creek terrane as a late Triassic-early Jurassic ophiolite mélange that was tilted and exposed during doming in the Neogene. The deepest part of the exposed Rattlesnake creek terrane, the Seiad complex, represents the ophiolitic basement of an island arc that was accreted to North America in the Jurassic (Garlick et al., 2009). This area, in the north central Klamath Mountains, is where our samples were collected. Metamorphosed rock compositions in the Seiad are primarily ultramafic, but there are also mafic, volcanic, and sedimentary units.

Petrographic features suggest low grade metasomatism occurred in the Seiad complex, probably while Seiad peridotites resided in the upper crust during imbrication (Frost, 1975; Coleman et al., 1988; Garlick et al., 2009). Following that, there was a high temperature interval where the complex experienced penetrative deformation (Garlick et al., 2009). The highest-grade conditions reported in the Klamath Mountains are in the Seiad Complex (Medaris, 1966, 1975; Lundquist, 1983; Grover, 1984; Grover and Rice, 1985; Lieberman and Rice, 1986; Snoke and Barnes, 2006) which includes rocks metamorphosed to the granulite facies (Garlick et al., 2009).

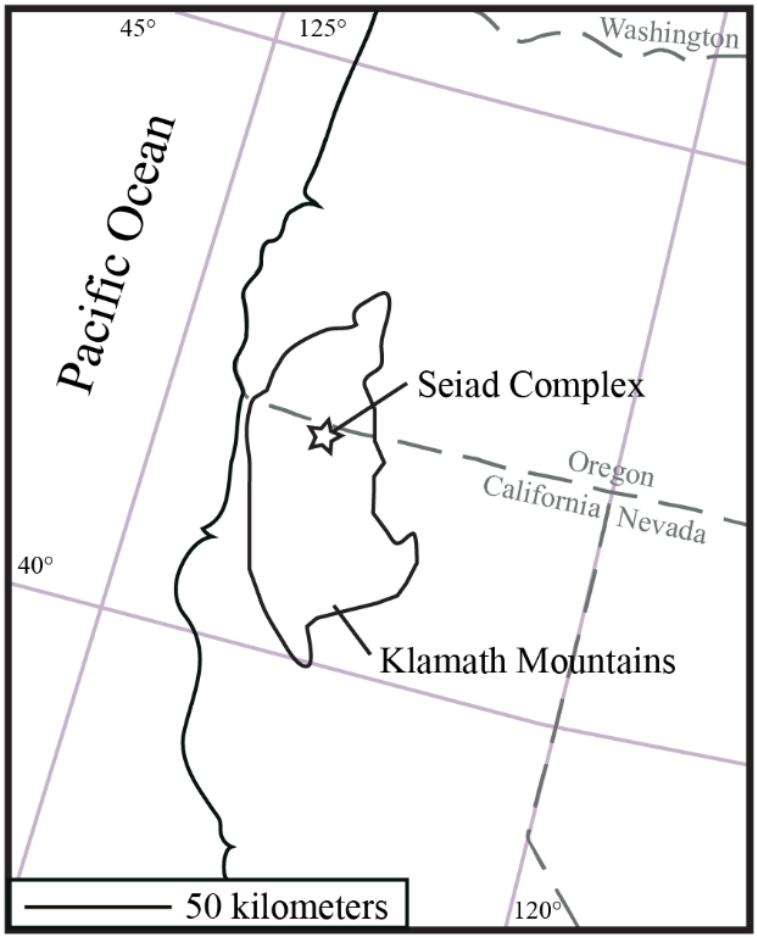

Figure 1. Regional location map of Klamath Mountains and Seiad Complex adapted from Garlick et al. (2009).

ANALYTICAL PROCEDURE

Mineral equilibria are used to estimate fugacities of oxygen and H_2O, an approach that requires independent estimates of T and P, which are also determined via the application of equilibria between minerals. This approach requires the characterization of the chemical compositions of co-existing minerals, and these compositions were determined using the CAMECA SX-5 Electron Microprobe (EMP) at Texas A&M University. Olivines, pyroxenes, and spinels were analyzed with a beam current of 20 nA, an accelerating voltage of 15 kV, and a beam diameter of 2 μm. Amphiboles were analyzed with a beam current of 10 nA, an accelerating voltage of 15 kV, and a beam diameter of 10 μm. In each sample, analyses were conducted on at least 3 different grains per slide with traverses of ten or more points across each grain.

Olivines and spinels were normalized to 3 cations, and pyroxenes were normalized to 4 cations. Unfortunately, conventional electron microprobe analyses are unable to differentiate between valence states of Fe. Olivines contain only small or trace amounts of Fe^{3+} (Ejima et al., 2018), and therefore $Fe^{3+}/\sum Fe = 0$ in normalized formulas (where $\sum Fe = Fe^{3+} + Fe^{2+}$). Values of $Fe^{3+}/\sum Fe$ were estimated via charge balance for pyroxenes and spinel. However, this approach may generate significant systematic errors (Woodland et al., 1992; Wood and Virgo, 1989). In the case of spinel, these inaccuracies can be corrected with access to secondary spinel standards for which $Fe^{3+}/\sum Fe$ values have been independently determined (Wood and Virgo, 1989). A suite of spinels with known $Fe^{3+}/\sum Fe$ were acquired (courtesy of B. Wood), and analyzed with the electron microprobe along with unknown spinels from the Seiad complex. The $Fe^{3+}/\sum Fe$ ratios of Seiad spinels estimated using charge balance were corrected using these secondary

standards (Wood and Virgo, 1989). Corrections to Fe^{3+} were less than .03 atoms per formula unit (apfu).

Although conventional EMP analyses do not yield a value of $Fe^{3+}/\sum Fe$, it is possible to quantify this value by relating the characteristics of FeLα peaks to Fe^{3+} contents (Hofer et al., 1994; Fialin et al., 2001). Lamb et al. (2012) applied this type of approach to amphiboles and demonstrated that the location of the FeLα peak changes as a function of $Fe^{3+}/\sum Fe$ and total Fe. Standards available from the calibration of Lamb et al. (2012) have FeO contents of 7.4-12.3 wt%, and this calibration should not be applied to FeO contents that are significantly outside this range (Lamb et al., 2012). The amphiboles analyzed for this study contained 3.5- 4.0 wt% FeO, outside the range of available amphibole standards. Therefore, in this study, Fe^{3+} in amphibole is set at zero; an approach that yields maximum aH_2O values when estimated using dehydration reactions (Kang et al., 2017). Furthermore, Kang et al. (2017) and Lamb and Popp (2009) demonstrated that changes to Fe oxidation may result in only small changes to aH_2O (< 0.1).

In addition to values of $Fe^{3+}/\sum Fe$, complete characterization of amphibole chemistry requires characterization of H_2 contents and A-site vacancies. Given a value of Fe^{3+} (measured or assumed), and the chemical characterization of an amphibole via conventional microprobe analyses, it is possible to estimate the OH^- contents of amphiboles using the correlation between cations and the components of the Z site (Popp et al., 1995). In this case, the sum of Ti^{4+} and Fe^{3+} is equivalent to the O-content of the Z-site, as illustrated by the equation:

$$2.00 = (Fe^{3+} + Ti^{4+}) + Cl^- + F^- + OH^- \quad (1)$$

where 2.00 is the sum of components in the Z site of an amphibole (Popp et al., 1995). The OH^- content can be calculated given the chemical composition of an amphibole.

To determine amphibole formulas, an iterative technique designed by Lamb and Popp (2009) was implemented. In the first iteration of the calculation, the formula is normalized to 24 oxygens. However, this step usually does not produce an amphibole formula that is charge balanced. To do so, the number of cations is reduced by a very small increment while their proportions are maintained, and then the oxy component is recalculated. This process is repeated until the total negative and positive charges are equal (charge balance).

SAMPLE DESCRIPTION

Five samples of spinel lherzolite were collected from the West Fork rock lherzolite and West Fork ultramafic body (Figure 2). Olivine, clinopyroxene, orthopyroxene, amphibole, and spinel were present in all samples. Optical estimates indicate olivine is the dominant mineral (55-75%), followed by pyroxene (15-30%), amphibole (5-20%) and spinel (<5%). Clinopyroxene generally accounted for 60 – 70% of the total amount of pyroxenes. Mineralogy and estimated mineral abundances are tabulated in the appendix.

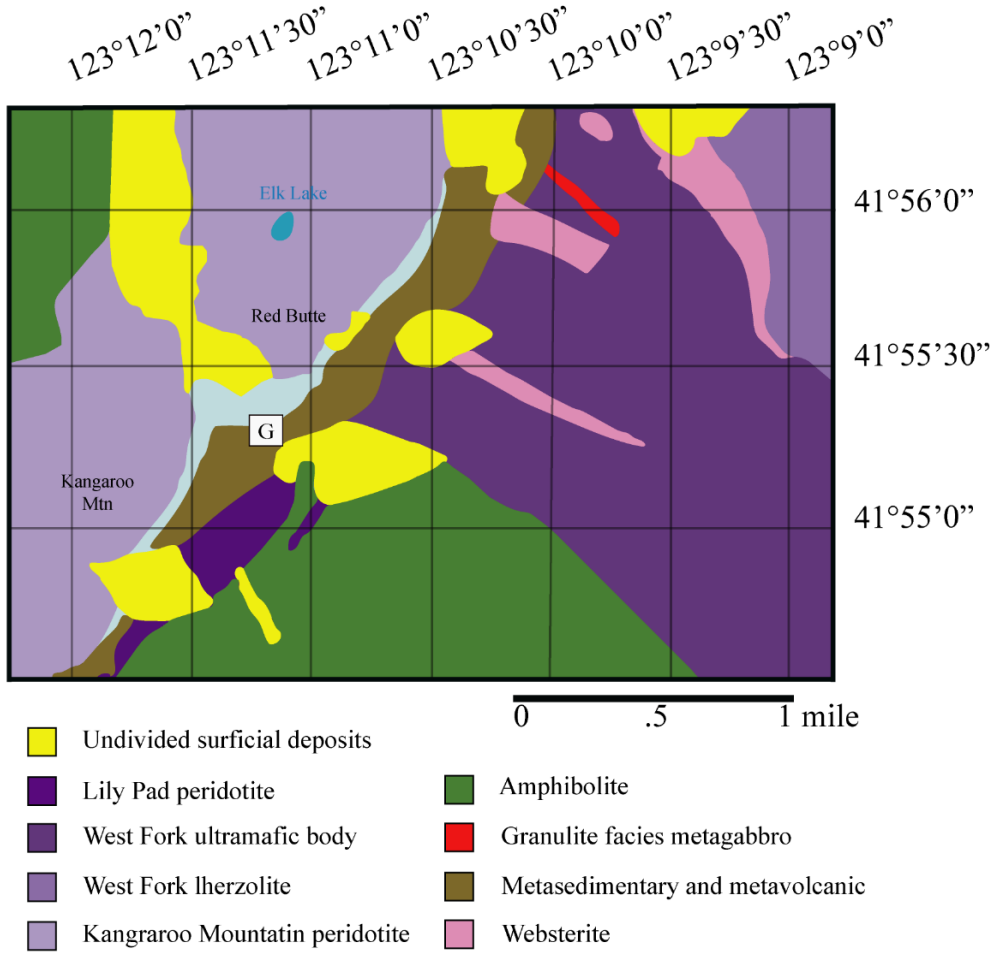

Figure 2. Geologic units of the Seiad complex in the vicinity of our samples adapted from Garlick et al. (2009). Location of a sample described by Garlick et al. (2009) is denoted by the letter "G".

Samples WSD1, WSD2, WSD3, and WSD4 are foliated and have roughly equal grain sizes (Figure 3a). WSD17, however, has coarser grains relative to other samples (Figure 3b). In addition, WSD2 and WSD3 contain orthopyroxene porphyroblasts that occur disseminated throughout the matrix (Figure 3c). WSD3 also contains coarse grains of orthopyroxene and amphibole localized into monomineralic bands (Figure 3d).

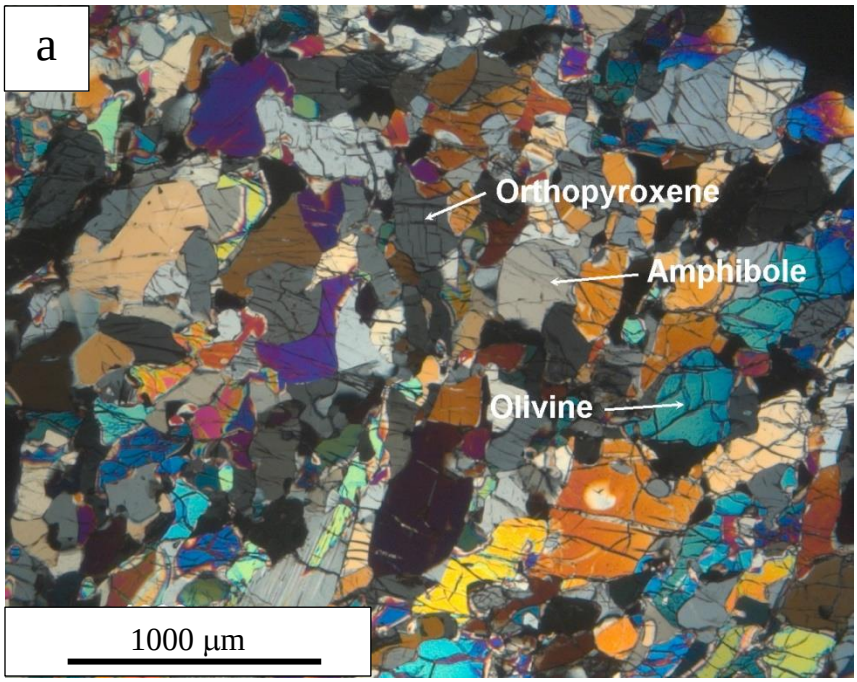

Figure 3. Examples of mineralogy and textures of samples from the West Fork ultramafic body. (a) Sample WSD1 is typical of various samples from the West Fork ultramafic body. It is foliated and contains amphibole, orthopyroxene, olivine, clinopyroxene (not pictured), and spinel (not pictured). (b) In contrast to other samples, WSD17 was courser grained and more dominantly olivine. (c) Samples WSD2 and WSD3 featured sparsely distributed large orthopyroxene grains. (d) Sample WSD3 featured distinctive monomineralic bands of both orthopyroxene and amphibole in addition to orthopyroxene and amphibole within the matrix.

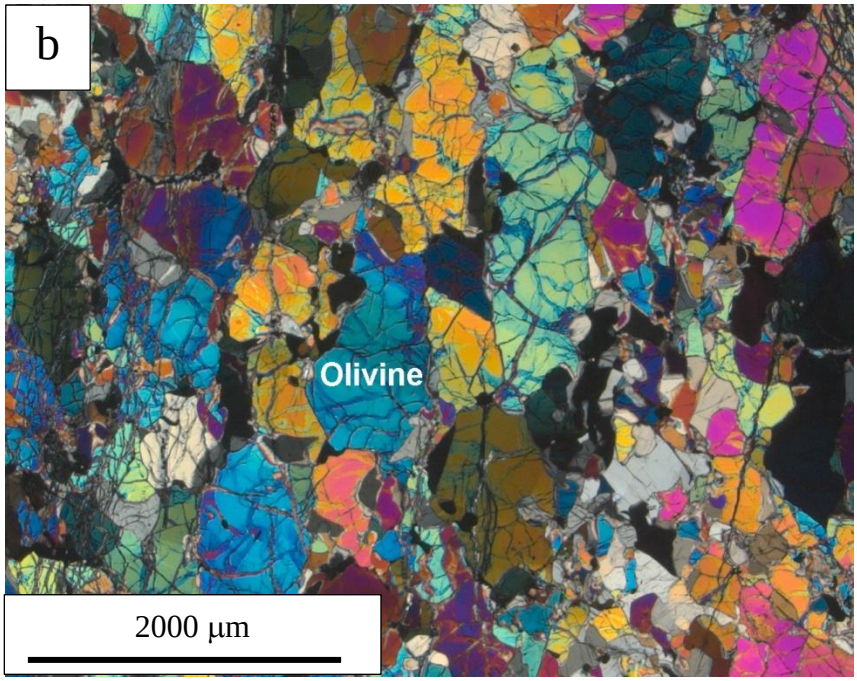

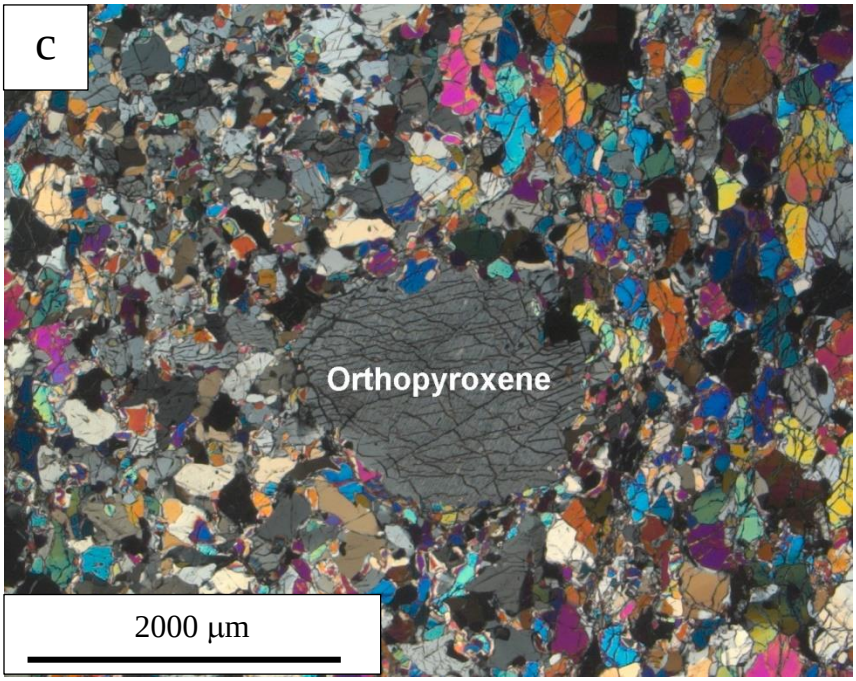

Figure 3. Continued

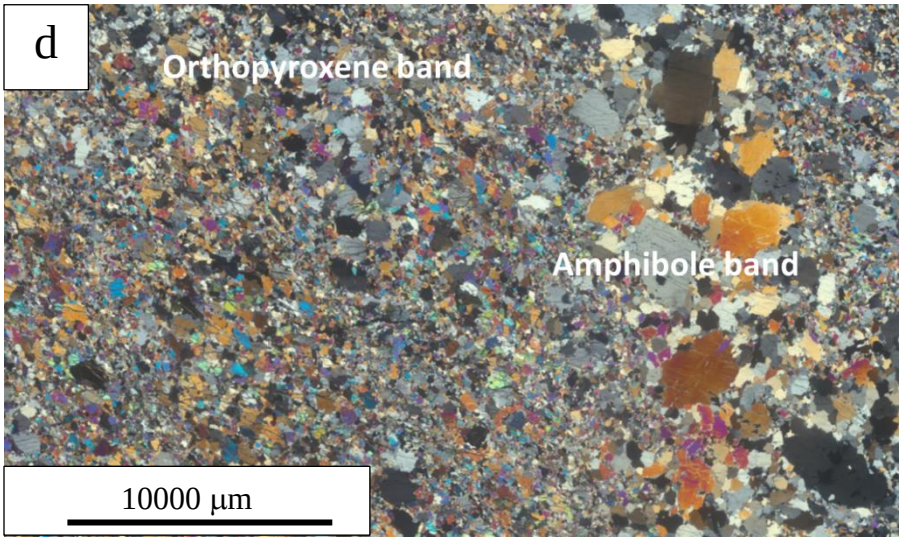

Figure 3. Continued

MINERAL CHEMISTRY

The range in Mg#'s (Mg/(Mg + Fe)) for olivine is 0.87 – 0.89, orthopyroxene is 0.89 – 0.93, clinopyroxene is 0.93 – 0.97, and spinel is 0.63 – 0.75. Values of $Fe^{3+}/\sum Fe$ were determined for spinel (0.04 – 0.15), and estimated via charge balance for orthopyroxene (0.04 – 0.27) and clinopyroxene (0.10 – 0.70). Chemical analyses of all samples are available in the appendix.

Olivine grains are chemically homogeneous from core to rim. However, other minerals typically have homogeneous central regions, but exhibit small compositional changes in close proximity (typically 10μm or less) to the rims. Clinopyroxene and amphibole grains generally exhibit nonconcentric decreases in Al and increases in Si and Mg content from the core to the rim of the grains (Figure 4a, b). Concentric zoning of these same elements was observed in orthopyroxene. In contrast, a different trend was observed in spinel grains, where Al increased, and Fe and Cr decreased towards the rims of most grains (Figure 4c).

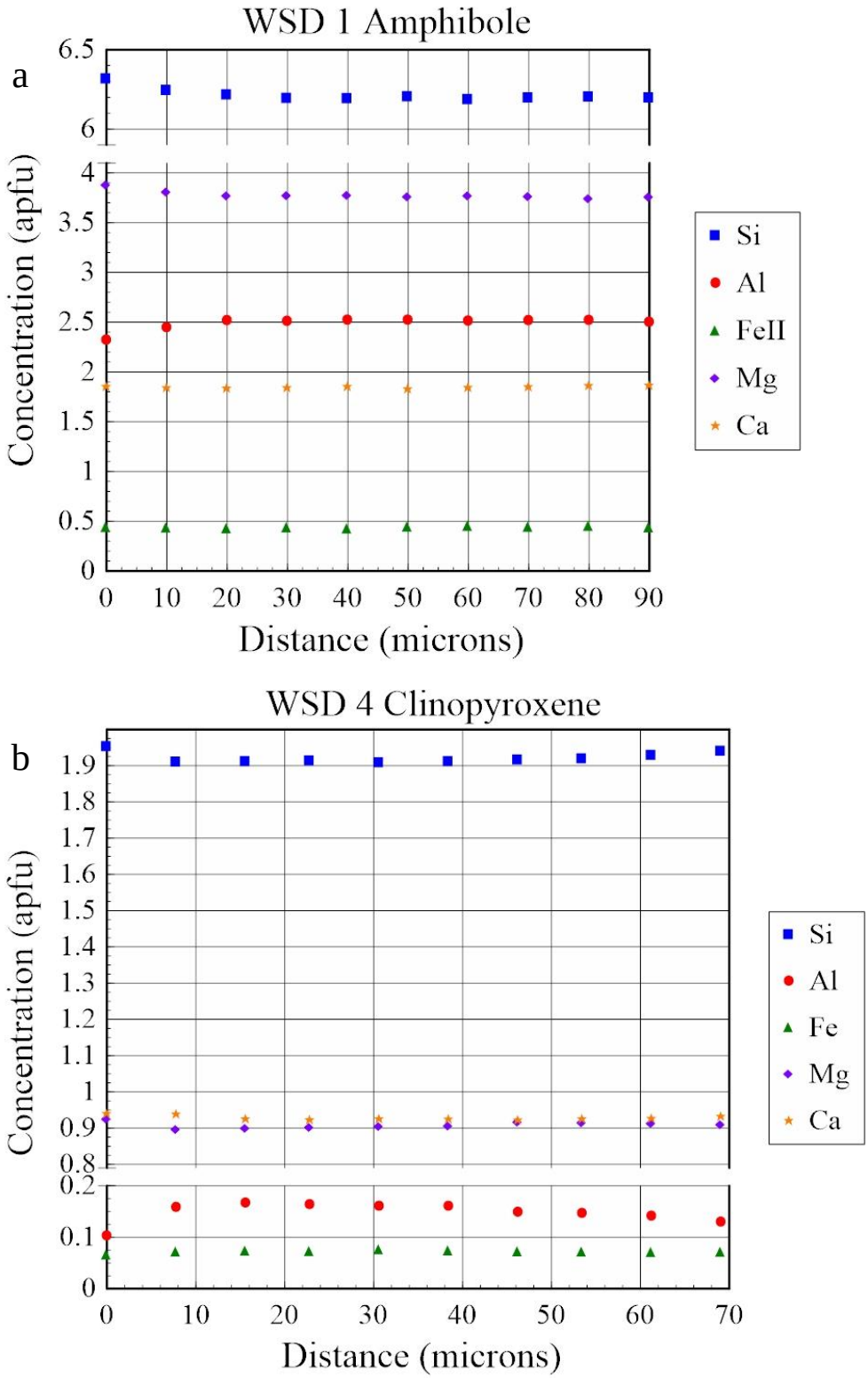

Figure 4. Chemical analyses from electron microprobe. Traverses across amphibole (a), clinopyroxene (b), and spinel (c) in these samples show two distinctive trends. First, in pyroxene and amphibole there is a small (< 0.1 apfu) decrease in Al, and an increase in Mg close (10μm) to the rim. Second, in spinel there is an increase in Al, and a decrease in Cr and Fe close to the rim.

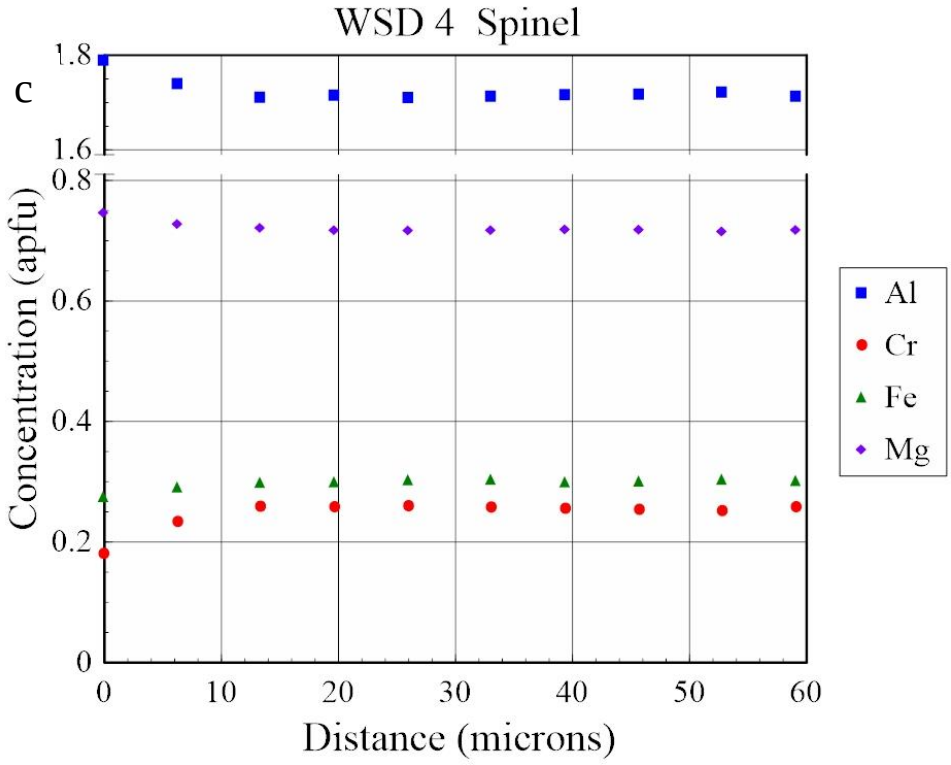

Figure 4. Continued.

TEMPERATURE AND PRESSURE

Temperatures ranging from 770°C to 810°C (Table 1) were estimated using the compositions of coexisting pyroxenes (Taylor, 1998). These temperatures are in good agreement with those determined by Garlick et al. (2009) for granulite-facies rocks in the Seiad (743±52°C). Garlick et al. (2009) also used a garnet barometer calibrated by Kohn and Spear (1989) and Taylor (1998) on lower grade rocks to calculate pressure and temperature conditions of 7.3 ± 0.9 kb at 700°C respectively. Furthermore, the minimum pressure at which spinel is stable in our samples is 6.5 kb at 740°C (calculated using the self-consistent data-base consistent with THERMOCALC (Holland and Powell, 2011)). In light of this lower limit, and based on calculated pressures and temperatures from Garlick et al. (2009), a pressure of 8 kb is used in this study.

Nimis and Grutter (2010) reviewed and evaluated a number of two-pyroxene and other geothermometers applicable to peridotites. They found the Taylor (1998) (T98) formulation of the two-pyroxene geothermometer best reproduced available data from relevant experiments and that the single pyroxene thermometer of Nimis and Taylor (2000) (NT) produced temperatures that agreed with Taylor (1998) to ± 30°C. In addition, Nimis and Grutter (2010) made empirical modifications to the Brey et al. (1990) Ca-in-OPX thermometer (BKNG) to produce a version that also agreed with Taylor (1998), in this case, to ±72°C (2 sigma).

Agreement between temperatures as estimated using these different thermometers is considered evidence that minerals in a given hand sample are in chemical equilibrium (Stachel et al., 2004; Lazarov et al., 2009; Nimis and Grutter, 2010). This approach is useful because the T98, BKNG, and NT thermometers depend on the compositions of clinopyroxene and orthopyroxene to differing degrees, and are, therefore, considered semi-independent temperature

estimates (Nimis and Grutter, 2010). T98 and NT are more heavily dependent on the composition of clinopyroxene while BKNG depends only on the composition of the co-existing orthopyroxene (Nimis and Grutter, 2010). The temperatures calculated from our samples using these three different two-pyroxene thermometers agree to within the uncertainties mentioned above (Table 1). Thus, these results are consistent with pyroxenes composition at or very close to equilibrium.

Temperatures were estimated using rim and core compositions of co-existing pyroxene grains and the Taylor (1998) thermometer , producing average temperatures of 770°C and 790°C respectively (see appendix). The differences between core and rim temperatures are relatively small; however, the difference is consistent with the interpretation that the small changes in mineral composition that occur near the rim may be the product of re-equilibration during retrograde metamorphism.

Table 1. Temperature estimates for Seiad samples (see text).

Sample:	BKNG	T98	NT
WSD1	764	**792**	810
WSD2	774	**769**	783
WSD3	757	**752**	768
WSD4	798	**802**	820
WSD17	849	**809**	833

DEHYDRATION EQUILIBRIA

A value of aH_2O can be estimated by writing equilibria between amphibole and other minerals present in our samples. These equilibria are typically expressed in terms of mineral endmembers (e.g. the enstatite endmember in orthopyroxene – $MgSiO_3$), and different equilibria may involve different mineral endmembers. In order to apply mineral equilibria to calculate aH_2O, the activities of the relevant endmembers must be determined. The uncertainty in determining the activity of an endmember usually decreases with increasing abundance of that endmember (Spear, 1993: pg 190; Lamb and Popp, 2009). Therefore, because mantle minerals are generally Mg-rich, Mg endmembers are preferred. In addition, the quality of activity-composition models may not be the same for all minerals within any particular paragenesis. Because the amphiboles in these lherzolites are Na-rich, and pyroxene activity models are relatively well developed, an equilibrium involving pargasite and jadeite may be particularly suitable for estimating values of aH_2O (Lamb and Popp, 2009). The complete reaction is:

$$2Parg + En = 2Fo + 4Di + 2Sp + 2Jd + 2H_2O \qquad (2)$$

$$2NaCa_2Mg_4Al_3Si_6O_{22}(OH)_2 + Mg_2Si_2O_6 =$$
$$2Mg_2SiO_4 + 4CaMgSi_2O_6 + 2MgAl_2O_4 + 2NaAlSi_2O_6 + 2H_2O$$

Kang et al. (2017), Lamb and Popp (2009), and Popp et al. (2006) applied this equilibrium to estimate values of aH_2O. This approach determined the stability of equilibrium (2) in terms of P, T, and aH_2O using the self-consistent thermodynamic data-base developed for use with THERMOCALC software (Powell et al., 1998). Multiple activity models were evaluated to determine mantle mineral activities. Activity models developed for use with

THERMOCALC were preferred because of the availability of existing amphibole models (Dale et al., 2005; Diener et al., 2007). However, Lamb and Popp (2009) also applied activity models consistent with the MELTS software package because these models were developed specifically for mantle rocks (Sack and Ghiorso, 1989, 1991, 1994). It was determined that different activity models (developed for both THERMOCALC and MELTS) produced small differences (generally < 0.1) when used to calculate the activities of Mg endmembers of olivine and clinopyroxene. For these same minerals, ideal activities were also calculated and found to be similar to non-ideal activities (generally differences were < .05). There were larger differences in the activities of orthopyroxene and spinel when different models were applied (generally < 0.3), however even considering these variations, estimations of aH_2O differed by less than 0.01 (Lamb and Popp, 2009). We have determined mantle mineral activities (Table 2) using the core compositions of olivine, clinopyroxene, orthopyroxene, and spinel, and a recent set of activity models calibrated specifically for ultramafic rocks (Jennings and Holland, 2015). In addition, three different amphibole activity-composition (a-X) models were applied (Diener and Powell, 2012; Green et al., 2016). One recent amphibole a-X model, presented by Green et al. (2016) was developed for the NA_2O-CaO-K_2O-FeO-MgO-Al_2O_3-SiO-H_2O-TiO_2-Fe_2O_3 system in meta-basic rocks. The model extended existing a-X formulations, such as that by Diener et al. (2007), by including Ti. However, no a-X model has been derived specifically for compositions typical of mantle amphiboles. Therefore, we compared three a-X models, including one ideal and two non-ideal models, to estimate the activity of pargasite in our amphiboles. In each model, the activity of pargasite was corrected for the OH- content (Lamb and Popp, 2009).

Average amphibole compositions were used when estimating the activities of endmembers using these three models developed (see appendix). Ideal activities of pargasite are,

on average, three times smaller than non-ideal activities. The non-ideal activities are similar to one another, although pargasite activities calculated using Green et al. (2016) are consistently lower, and the average difference between these non-ideal activities is 0.03 (Table 2).

Table 2. Activities of mineral endmembers from reaction 2.

Sample	a_{Di}	a_{Jd}	a_{Fo}	a_{Sp}	a_{En}	a_{Parg}		
						Ideal	G16	D12
WSD1	0.80	0.02	0.80	0.65	0.76	0.08	0.21	0.25
WSD2	0.80	0.02	0.81	0.66	0.77	0.07	0.28	0.31
WSD3	0.85	0.00	0.80	0.59	0.76	0.04	0.08	0.09
WSD4	0.81	0.01	0.82	0.64	0.76	0.09	0.22	0.24
WSD17	0.79	0.01	0.82	0.64	0.77	0.04	0.18	0.22

G16 = Green et al. (2016), D12 = Diener and Powell (2012)

Activities of H_2O were calculated using pargasite activities generated from both non-ideal models (Table 3) using dataset 6.2 in THERMOCALC (Holland and Powell, 2011). Application of equilibrium (2), using pargasite activities from Diener and Powell (2012), returned values ranging from 0.29 to 0.59. The same equilibrium produced slightly lower values of aH_2O, ranging from 0.26 to 0.52, when pargasite activities were estimated using Green et al. (2016). To evaluate the range in uncertainty of aH_2O calculated for each sample using dehydration equilibria, values of aH_2O were recalculated at temperatures 30°C above and below temperatures estimated using the Taylor (1998) thermometer, which is the range in uncertainty given by Taylor (1998). Uncertainties in calculated aH_2O for each sample were also assessed by recalculating aH_2O using a pressure of 7 kb. Samples had an average uncertainty in aH_2O of ± 0.04.

Table 3. Activities of H_2O.

Sample	aH_2O	
	Green et al. (2016)	Diener and Powell (2012)
WSD1	0.29	0.33
WSD2	0.26	0.29
WSD3	0.52	0.59
WSD4	0.41	0.43
WSD17	0.31	0.37

OXYGEN FUGACITY

Several calibrations of fO_2 barometers have been proposed (O'Neill and Wall, 1987; Mattioli and Wood, 1988; Nell and Wood, 1991; Ballhaus et al., 1991; Miller et al., 2016). Most of these oxy-barometers are based on the equilibria:

$$6Fe_2SiO_4 + O_2 = 3Fe_2Si_2O_6 + 2Fe_3O_4 \qquad (3)$$

although the Miller et al. (2016) oxy-barometer considers three different oxygen-buffering equilibria simultaneously.

Wood (1990) and Miller et al. (2016) were used to calculate oxygen fugacities for our samples (Table 4). The majority (4 out of 5) of oxygen fugacities calculated using Miller et al. (2016) were more oxidizing than oxygen fugacities calculated using Wood (1990). Analyses that were calculated with Miller et al. (2016) ranged from -2.30 – 0.36 log units relative to the FMQ buffer ($\Delta\log fO_2$ (FMQ)). Those oxygen fugacities that were calculated with Wood (1990) ranged from -2.22 – 0.40 $\Delta\log fO_2$ (FMQ). Uncertainties in fO_2 were found to be ± 0.35 $\Delta\log fO_2$ (FMQ) by Wood (1990).

Table 4. Fugacities of oxygen relative to the FMQ buffer.

Sample	$\Delta\log fO_2$ (FMQ)	
	Wood	Miller
WSD1	-0.95	-0.48
WSD2	-2.01	-1.81
WSD3	0.02	0.36
WSD4	-1.82	-1.76
WSD17	-0.88	-0.98

C-O-H FLUID EQUILIBRIA

If a lithostatically-pressured fluid phase exists along grain boundaries of peridotites in the upper mantle, fluid inclusion, C-isotope studies, and calculation of fluid speciation in the C-O-H system suggest that CO_2 and, possibly CH_4, may constitute the major species (Frezzotti and Touret, 2014; Deines, 1980; Andersen et al., 1984). Lithostatically pressured fluids that characterize granulite-facies metamorphism, if present, are thought by some to be CO_2-rich and/or brines (Newton et al., 1998; Santosh and Omori, 2008b; Touret and Huizenga, 2012). However, granulite-facies fluids are likely heterogeneous and some rocks were fluid absent at the peak of metamorphism (Lamb and Valley, 1984, 1985; Edwards and Essene, 1988). Several studies have used equilibria involving C-O-H fluid species in mantle rocks to assess the nature of fluids in the deep crust and upper mantle, and, in some cases, determine if a lithostatically pressured C-O-H fluid phase was present (Lamb and Valley, 1984, 1985; Lamb and Popp, 2009; Kang et al., 2017; Hunt, 2017).

At elevated pressures and temperatures, the major components of fluid in the C-O-H system are typically CO_2, H_2O, and CH_4, while the minor species consist of O_2, H_2, and CO (French, 1966; Ohmoto and Kerrick, 1977; Lamb and Valley, 1984). In the presence of graphite or diamond (C), these fluid species can be related by the following equilibria:

$$C + O_2 = CO_2 \qquad (4)$$

$$C + \frac{1}{2}O_2 = CO \qquad (5)$$

$$H_2 + \frac{1}{2}O_2 = H_2O \qquad (6)$$

$$C + 2H_2 = CH_4 \qquad (7)$$

It has been argued that a fluid present at grain boundaries will be lithostatically pressured at the depths of the upper mantle due to closure of pores in solids at high temperature and pressure (Walther and Orville, 1982; Wood and Walther, 1983; Spear, 1993: pg 707). If a free fluid is present, the fluid pressure (P_F) is equal to the sum of the partial pressures of its components, and if P_F = lithostatic pressure (P_L), then:

$$P_L = P_F = P_{H_2O} + P_{CO_2} + P_{CH_4} + P_{CO} + P_{H_2} + P_{O_2} \qquad (8)$$

Most studies employ six major species (French, 1966; Ohmoto and Kerrick, 1977; Lamb and Valley, 1984; Huizenga, 2001). However, other species may be included, such as C_2H_6, which was included by Zhang and Duan (2009). In this case, a fifth equilibrium can be written as:

$$2C + 3H_2 = C_2H_6 \qquad (9)$$

and a modification to include PC_2H_6 must also be made to Equation 8.

Equations 4 through 8 (or 9) can be solved simultaneously if fO_2 (or the fugacity of some other fluid species) is fixed in the presence of graphite/diamond (i.e. the activity of Carbon (aC) = 1), and P_L=P_F (French, 1966; Ohmoto and Kerrick, 1977; Lamb and Valley, 1984). In addition, in some cases the condition aC = 1 may still be applied if graphite or diamond is not present (Lamb and Valley, 1984, 1985). The effect would be to minimize aH_2O values and maximize CO_2 and CH_4 values in the range of fO_2 where graphite or diamond is stable (Lamb and Popp, 2009). If the fugacities of two fluid phases can be fixed, it is possible to solve for the fugacities

of the remaining fluid species at a given value of aC without application of equation (8), and, therefore, in these cases it is not necessary to assume the presence of a lithostatically pressured fluid phase (Lamb and Valley, 1984, 1985). For example, given values of aH_2O and fO_2 estimated from mineral equilibria, it is possible to solve for the fugacities of all fluid species in the C-O-H system, at which point, fluid pressure could then be calculated from equation (8), and compared to lithostatic pressure. Fixing the value of aC = 1 yields a maximum value for fluid pressure. If P_F is significantly less than P_L, this suggests that no free-fluid phase is present unless the fluid contains a significant amount non-C-O-H species (e.g. N_2 - or S-species). The presence of a non-C-O-H species has been observed in fluid inclusions from some samples (Kreulen and Schuiling, 1982; Andersen et al., 1984). However, these instances are relatively rare.

In our samples, values of aH_2O estimated from dehydration equilibrium (2) are compared to values estimated from C-O-H equilibria for those samples in which the values of fO_2 fall within the graphite stability (Figure 5). Figure 5 illustrates that, at any given oxygen fugacity, the constraint aC = 1 yields a minimum limit for aH_2O (Figure 5a), and that a lower value aC will result in greater activities of H_2O and lower activities of CO_2 and CH_4 (Figure 5b). When aC = 1, minimum values of aH_2O calculated from C-O-H equilibria ranged from 0.47 – 0.86, and most of these were significantly higher than those calculated using dehydration equilibria (Table 5). These contradicting results indicate that the assumption $P_L = P_F$ is not valid, and argue against the presence of a lithostatically pressured fluid phase in at least three of our samples (Kang et al., 2017).

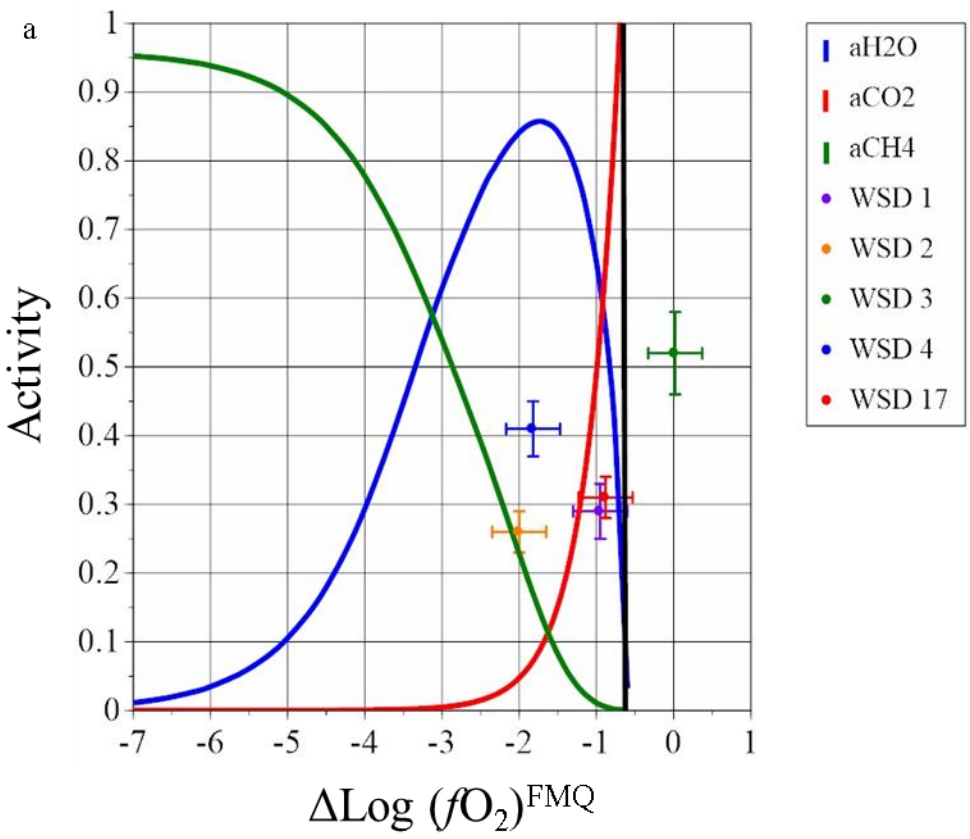

Figure 5. Activities of major fluid species. Values of aH_2, aCO_2, aCH_4, and aH_2O vary as a function of log fO_2 relative to FMQ at (a) aC = 1 and (b) aC = 0.01, 790°C and 8 kbar. Values of fO_2 and aH_2O from dehydration equilibria for all samples are plotted along with values of aH_2O from C-O-H equilibria for comparison. Low activity species were omitted to increase figure clarity. The black line indicates the limit of graphite stability.

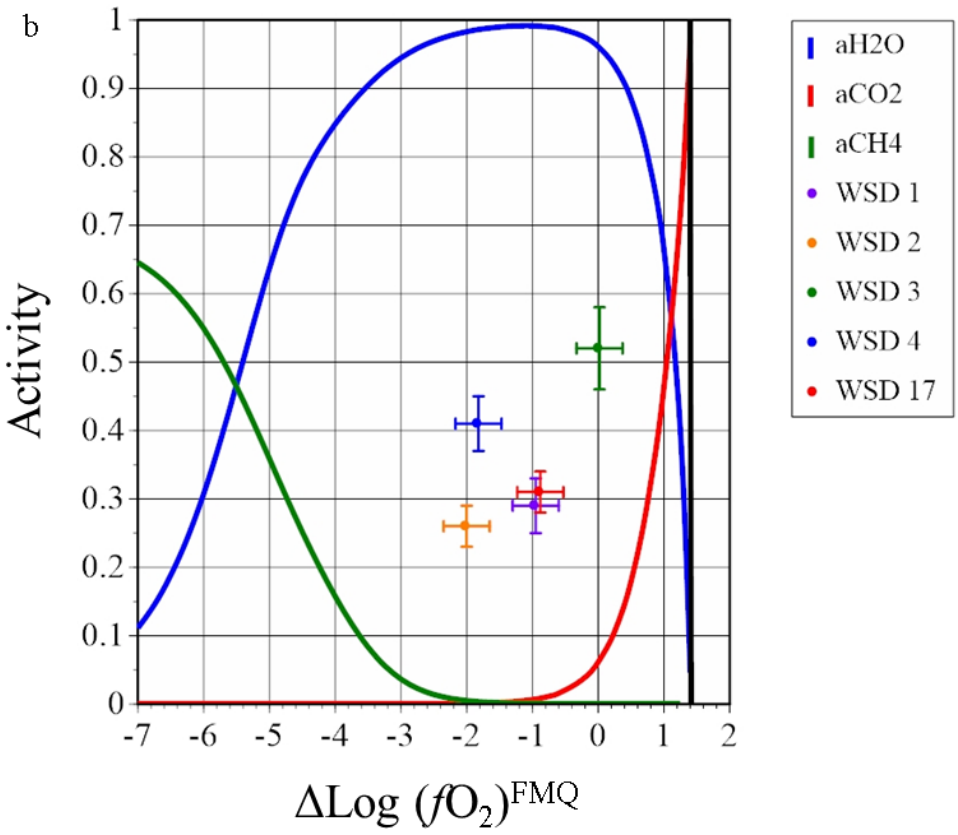

Figure 5. Continued.

Table 5. Activities of H_2O calculated from different methods.

		aH_2O	
Sample	Dehydration	C-O-H	
		aC = 1	aC = .01
WSD1	0.29	0.52	0.99
WSD2	0.26	0.78	0.98
WSD3	0.52	*	0.96
WSD4	0.41	0.86	0.99
WSD17	0.31	0.47	0.99

* = oxygen fugacity inconsistent with graphite stability

DISCUSSION AND IMPLICATIONS

Values of aH_2O estimated from dehydration equilibria range from approximately 0.3 to 0.6. Clearly, the presence of amphibole does not require the presence of lithostatically-pressured fluids, an H_2O-rich fluid, nor does it imply conditions are especially "wet". This result is consistent with previous studies of mantle peridotites (Lamb and Popp, 2009; Kang et al., 2017), and crustal rocks metamorphosed to granulite-facies conditions (Lamb and Valley, 1984, 1985).

Values of oxygen fugacity estimated for Seiad peridotites exhibit significant variation between samples and, with the exception of WSD3, are significantly below the FMQ buffer. According to studies such as Wood et al. (1990), Woodland et al. (1992), and Woodland and Koch (2003) these values are within the range of redox conditions recorded for the upper mantle range (-3.0 to 2 log units relative to FMQ).

The values of aH_2O reported here are significantly less than 1, which is consistent with previous results for rocks metamorphosed under granulite-facies conditions (Valley et al., 1983; Lamb and Valley, 1984; Powers and Bohlen, 1985). These low values of aH_2O may be generated by one or more of three different processes: (1) removal of H_2O via partial melting (Powell, 1983; Valley et al., 1990; Valley, 1992), (2) infiltration of a low aH_2O fluid such as CO_2 (Santosh and Omori, 2008a) or brine (Aranovich and Newton, 1996; Newton et al., 1998; Kumar, 2004), or (3) recrystallization of a low aH_2O (dry) protolith.

The presence of high-density CO_2 inclusions have been used to explain low values of aH_2O in granulite-facies rocks (Hollister and Burruss, 1976; Coolen, 1982; Touret and Dietvorst, 1983; Hansen et al., 1984; Rudnick et al., 1984; Santosh, 1985; Schreurs, 1984). In addition, based on the presence of CO_2-rich fluid inclusions in mantle peridotites, it has been argued that the uppermost mantle is characterized by the presence of CO_2-rich fluids (Frezzotti and Touret,

2014), and that this mantle CO_2 may ultimately be transferred to the lower crust, driving granulite-forming reactions (Touret, 1971; Touret, 1992; Santosh and Omori, 2008a). However, other studies have demonstrated that CO_2-rich fluid inclusions in high-grade rocks do not contain pristine samples of the peak metamorphic fluid. These studies include characterization of CO_2-rich fluid inclusions in rocks in which mineral equilibria indicate that the peak metamorphic fluid, if present, could not be CO_2-rich (Lamb et al., 1987; Lamb et al., 1991; Lamb and Morrison, 1997; Lamb, 2005). Values of fO_2 estimated for the Seiad peridotites are inconsistent with the presence of a CO_2-rich fluid. Furthermore, the inconsistency between values of aH_2O estimated from simultaneous solution of equilibria in the C-O-H system and values of aH_2O estimated from dehydration equilibria suggests that P_{Fluid} does not equal $P_{Lithostatic}$. Thus, there was no lithostatically-pressured fluid phase (e.g., wetting the grain boundaries), or the fluid phase was dominated by non-C-O-H fluid species.

Prior to being incorporated into the crust and metamorphosed under granulite facies conditions, the Seiad peridotites were part of the mantle. Consequently, information concerning the nature of mantle fluids may provide some insight into the nature of fluids in the Seiad peridotites prior to granulite-facies metamorphism. Two methods, among several that have been employed to investigate the nature of fluids in the upper mantle are: (1) measurement of the H-content in nominally anhydrous phases (NAMs), and (2) the application of fluid-buffering mineral equilibria. The hydrogen (H) contents of NAMs in peridotite xenoliths have been determined using various analytical techniques (Li et al., 2008; Skogby, 2006; Peslier, 2010; Warren and Hauri, 2014), and these analyses show mantle pyroxenes generally contain between 30 and 960 wt ppm H_2O, and mantle olivines typically range between 0 and 300 wt ppm H_2O (Skogby, 2006; Beran and Libowitzky, 2006; Peslier et al., 2010; Peslier et al., 2017). In many

cases, such as with Lamb and Popp (2009), the NAMs are not fluid saturated with respect to H_2O, consistent with values of aH_2O less than one. Dehydration equilibria have also been used to provide independent estimates of aH_2O in mantle rocks. These studies yield values of aH_2O which range from 0.02 – 0.4 (Lamb and Popp, 2009; Popp et al., 2006; Kang et al., 2017; Hunt, 2017).

Given that many mantle rocks may typically record values of aH_2O that are significantly less than 1, there is no need to invoke a mechanism such as partial melting, or the infiltration of a low aH_2O fluid, to explain low activities of H_2O during granulite facies metamorphism of the Seiad peridotites. Rather, it is likely that granulite-facies metamorphism simply involved recrystallization of already dry rocks. Where other lithologies are present, other mechanisms may have operated, and there is evidence of orthopyroxene formation via reaction involving partial melting in some rocks (Figure 6). However, the portion of the Seiad complex that experienced granulite facies metamorphism is dominated by peridotites (Figure 2) and, therefore, recrystallization of already dry rock was likely the dominant mechanism for generating low water activities.

Figure 6. A sample from the unit mapped as Metavolcanic and Metasedimentary (see Fig. 2). Large grains of orthopyroxene are rimmed by amphibole within a felsic segregation. This texture is consistent with a melting reaction that produced the orthopyroxene (opx) and felsic segregation. This melt would consume any available H_2O. Upon cooling and crystallization, this melt would lose dissolved H_2O that then reacts with the opx and produces the rimming amphibole.

SUMMARY

Mineral equilibria yield low values of aH_2O in granulite-facies rocks. Values of fO_2 preclude the infiltration of a CO_2-rich fluid, and C-O-H equilibria indicate the absence of a lithostatically pressured C-O-H fluid in at least three samples. Based on the mantle origin of these rocks, and the estimations of water content for the upper mantle, it is probable that these rocks represent granulite-facies metamorphism of dry mantle rocks.

REFERENCES

Andersen, T., S. Y. Oreilly, and W. L. Griffin. 1984. 'The Trapped Fluid Phase in Upper Mantle Xenoliths from Victoria, Australia - Implications for Mantle Metasomatism', *Contributions to Mineralogy and Petrology*, 88: 72-85.

Aranovich, L. Y., A. R. Makhluf, C. E. Manning, and R. C. Newton. 2014. 'Dehydration melting and the relationship between granites and granulites', *Precambrian Research*, 253: 26-37.

Aranovich, L. Y., and R. C. Newton. 1996. 'H2O activity in concentrated NaCl solutions at high pressures and temperatures measured by the brucite-periclase equilibrium', *Contributions to Mineralogy and Petrology*, 125: 200-12.

———. 1997. 'H2O activity in concentrated KCl and KCl-NaCl solutions at high temperatures and pressures measured by the brucite-periclase equilibrium', *Contributions to Mineralogy and Petrology*, 127: 261-71.

Ballhaus, C., R. F. Berry, and D. H. Green. 1991. 'High-Pressure Experimental Calibration of the Olivine-Ortho-Pyroxene-Spinel Oxygen Geobarometer - Implications for the Oxidation-State of the Upper Mantle', *Contributions to Mineralogy and Petrology*, 107: 27-40.

Beran, A., and E. Libowitzky. 2006. 'Water in natural mantle minerals II: Olivine, garnet and accessory minerals', *Water in Nominally Anhydrous Minerals*, 62: 169-91.

Brey, G. P., T. Kohler, and K. G. Nickel. 1990. 'Geothermobarometry in 4-Phase Lherzolites .1. Experimental Results from 10 to 60 Kb', *Journal of Petrology*, 31: 1313-52.

Clemens, J. D., and J. M. Watkins. 2001. 'The fluid regime of high-temperature metamorphism during granitoid magma genesis', *Contributions to Mineralogy and Petrology*, 140: 600-06.

Clemens, John D. 2006. "Melting of the continental crust; fluid regimes, melting reactions, and source rock fertility." In *Evolution and differentiation of the continental crust*, edited by Michael Brown and Tracy Rushmer, 296-330. Cambridge University Press, New York, NY, United States.

Coleman, R. G., C. E. Manning, N. Mortimer, M. M. Donato, and L. B. Hill. 1988. 'Tectonic and regional metamorphic framework of the Klamath Mountains and adjacent Coast Ranges, California and Oregon, in Ernst, W.G., ed.', *Metamorphism and crustal evolution of the western United States -- Rubey Volume*.

Condie, K. C., P. Allen, and B. L. Narayana. 1982. 'Geochemistry of the Archean Low-Grade to High-Grade Transition Zone, Southern India', *Contributions to Mineralogy and Petrology*, 81: 157-67.

Coolen, J. J. M. M. M. 1982. 'Carbonic fluid inclusions in granulites from Tanzania; a comparison of geobarometric methods based on fluid density and mineral chemistry', *Chemical Geology*, 37: 59-77.

Dale, J., R. Powell, R. W. White, F. L. Elmer, and T. J. B. Holland. 2005. 'A thermodynamic model for Ca-Na clinoamphiboles in Na2O-CaO-FeO-MgO-Al2O3-SiO2-H2O-O for petrological calculations', *Journal of Metamorphic Geology*, 23: 771-91.

Deines, P. 1980. 'The Carbon Isotopic Composition of Diamonds - Relationship to Diamond Shape, Color, Occurrence and Vapor Composition', *Geochimica et Cosmochimica Acta*, 44: 943-61.

Diener, J. F. A., and R. Powell. 2012. 'Revised activity-composition models for clinopyroxene and amphibole', *Journal of Metamorphic Geology*, 30: 131-42.

Diener, J. F. A., R. Powell, R. W. White, and T. J. B. Holland. 2007. 'A new thermodynamic model for clino- and orthoamphiboles in the system Na2O-CaO-FeO-MgO-Al2O3-SiO2-H2O-O', *Journal of Metamorphic Geology*, 25: 631-56.

Edwards, R. L., and E. J. Essene. 1988. 'Pressure, Temperature and C-O-H Fluid Fugacities across the Amphibolite Granulite Transition, Northwest Adirondack Mountains, New-York', *Journal of Petrology*, 29: 39-72.

Ejima, T., Y. Osanai, M. Akasaka, T. Adachi, N. Nakano, Y. Kon, H. Ohfuji, and J. Sereenen. 2018. 'Oxidation States of Fe in Constituent Minerals of a Spinel Lherzolite Xenolith from the Tariat Depression, Mongolia: The Significance of Fe3+ in Olivine', *Minerals*, 8.

Fialin, M., C. Wagner, N. Metrich, E. Humler, L. Galoisy, and A. Bezos. 2001. 'Fe3+/Sigma Fe vs. FeL alpha peak energy for minerals and glasses: Recent advances with the electron microprobe', *American Mineralogist*, 86: 456-65.

French, B. M. 1966. 'Some Geological Implications of Equilibrium between Graphite and a C - H - O Gas Phase at High Temperatures and Pressures', *Reviews of Geophysics*, 4: 223-&.

Frezzotti, M. L., and J. L. R. Touret. 2014. 'CO2, carbonate-rich melts, and brines in the mantle', *Geoscience Frontiers*, 5: 697-710.

Friend, C. R. L. 1985. 'Evidence for Fluid Pathways through Archean Crust and the Generation of the Closepet Granite, Karnataka, South-India', *Precambrian Research*, 27: 239-50.

Frost, B. R. 1975. 'Contact Metamorphism of Serpentinite, Chloritic Blackwall and Rodingite at Paddy-Go-Easy Pass, Central Cascades, Washington', *Journal of Petrology*, 16: 272-313.

Fyfe, W. S. 1973. 'Granulite Facies Partial Melting and Archaean Crust', *Philosophical Transactions of the Royal Society a-Mathematical Physical and Engineering Sciences*, 273: 457-61.

Gaetani, G. A., and T. L. Grove. 1998. 'The influence of water on melting of mantle peridotite', *Contributions to Mineralogy and Petrology*, 131: 323-46.

Garlick, S. R., L. G. Medaris, A. W. Snoke, J. J. Schwartz, and S. M. Swapp. 2009. 'Granulite- to amphibolite-facies metamorphism and penetrative deformation in a disrupted ophiolite, Klamath Mountains, California: A deep view into the basement of an accreted oceanic arc', *Crustal Cross Sections from the Western North American Cordillera and Elsewhere: Implications for Tectonic and Petrologic Processes*, 456: 151-86.

Green, E. C. R., R. W. White, J. F. A. Diener, R. Powell, T. J. B. Holland, and R. M. Palin. 2016. 'Activity-composition relations for the calculation of partial melting equilibria in metabasic rocks', *Journal of Metamorphic Geology*, 34: 845-69.

Grove, T. L., C. B. Till, and M. J. Krawczynski. 2012. 'The Role of H2O in Subduction Zone Magmatism', *Annual Review of Earth and Planetary Sciences, Vol 40*, 40: 413-39.

Grover, T. W. 1984. 'Progressive metamorphism west of the Condrey Mountain dome, north-central Klamath Mountains, northern California [M.S. thesis]', *Eugene, University of Oregon*: 129.

Grover, T. W., and J. M. Rice. 1985. 'A progressive metamorphic sequence west of the Condrey Mountain dome, north-central Klamath Mountains, California: Geological Society of America Abstracts with Programs ', 17: 358.

Hansen, E. C., R. C. Newton, and A. S. Janardhan. 1984. 'Fluid Inclusions in Rocks from the Amphibolite-Facies Gneiss to Charnockite Progression in Southern Karnataka, India - Direct Evidence Concerning the Fluids of Granulite Metamorphism', *Journal of Metamorphic Geology*, 2: 249-64.

Hirth, G., and D. L. Kohlstedt. 1996. 'Water in the oceanic upper mantle: Implications for rheology, melt extraction and the evolution of the lithosphere', *Earth and Planetary Science Letters*, 144: 93-108.

Hofer, H. E., G. P. Brey, B. Schulzdobrick, and R. Oberhansli. 1994. 'The Determination of the Oxidation-State of Iron by the Electron-Microprobe', *European Journal of Mineralogy*, 6: 407-18.

Holland, T. J. B., and R. Powell. 2011. 'An improved and extended internally consistent thermodynamic dataset for phases of petrological interest, involving a new equation of state for solids', *Journal of Metamorphic Geology*, 29: 333-83.

Hollister, L. S., and R. C. Burruss. 1976. 'Phase-Equilibria in Fluid Inclusions from Khtada Lake Metamorphic Complex', *Geochimica et Cosmochimica Acta*, 40: 163-75.

Huizenga, J. M. 2001. 'Thermodynamic modelling of C-O-H fluids', *Lithos*, 55: 101-14.

Hunt, Lindsey E. 2017. 'Application of mineral equilibria to constrain the nature of mantle fluids using mantle xenoliths'.

Janardhan, A. S., R. C. Newton, and E. C. Hansen. 1982. 'The Transformation of Amphibolite Facies Gneiss to Charnockite in Southern Karnataka and Northern Tamil-Nadu, India', *Contributions to Mineralogy and Petrology*, 79: 130-49.

Jennings, E. S., and T. J. B. Holland. 2015. 'A Simple Thermodynamic Model for Melting of Peridotite in the System NCFMASOCr', *Journal of Petrology*, 56: 869-92.

Kang, P., W. M. Lamb, and M. Drury. 2017. 'Using mineral equilibria to estimate H2O activities in peridotites from the Western Gneiss Region of Norway', *American Mineralogist*, 102: 1021-36.

Kohn, M. J., and F. S. Spear. 1989. 'Empirical Calibration of Geobarometers for the Assemblage Garnet + Hornblende + Plagioclase + Quartz', *American Mineralogist*, 74: 77-84.

Kreulen, R., and R. D. Schuiling. 1982. 'N2-Ch4-Co2 Fluids during Formation of the Dome De Lagout, France', *Geochimica et Cosmochimica Acta*, 46: 193-203.

Kumar, G. R. R. 2004. 'Mechanism of arrested charnockite formation at Nemmara, Palghat region, southern India', *Lithos*, 75: 331-58.

Lamb, W. 2005. *Carbonates in feldspathic gneisses from the granulite facies: implications for the formation of CO2-rich fluid inclusions* (Atlantic Publishers and Distributors: Metamorphism and Crustal Evolution).

Lamb, W. M., P. E. Brown, and J. W. Valley. 1991. 'Fluid Inclusions in Adirondack Granulites - Implications for the Retrograde P-T Path', *Contributions to Mineralogy and Petrology*, 107: 472-83.

Lamb, W. M., R. Guillemette, R. K. Popp, S. J. Fritz, and G. J. Chmiel. 2012. 'Determination of Fe3+/Fe using the electron microprobe: A calibration for amphiboles', *American Mineralogist*, 97: 951-61.

Lamb, W. M., and J. Morrison. 1997. 'Retrograde fluids in the Archean Shawmere anorthosite, Kapuskasing Structural Zone, Ontario, Canada', *Contributions to Mineralogy and Petrology*, 129: 105-19.

Lamb, W. M., and R. K. Popp. 2009. 'Amphibole equilibria in mantle rocks: Determining values of mantle a(H2O) and implications for mantle H2O contents', *American Mineralogist*, 94: 41-52.

Lamb, W. M., and J. W. Valley. 1988. 'Granulite Facies Amphibole and Biotite Equilibria, and Calculated Peak-Metamorphic Water Activities', *Contributions to Mineralogy and Petrology*, 100: 349-60.

Lamb, W. M., J. W. Valley, and P. E. Brown. 1987. 'Post-Metamorphic Co2-Rich Fluid Inclusions in Granulites', *Contributions to Mineralogy and Petrology*, 96: 485-95.

Lamb, W., and J. W. Valley. 1984. 'Metamorphism of Reduced Granulites in Low-Co2 Vapor-Free Environment', *Nature*, 312: 56-58.

———. 1985. 'C-O-H fluid calculations and granulite genesis', *The Deep Proterozoic Crust in the North Atlantic Provinces NATO ASI Series*, 158: 119-31.

Lazarov, M., A. B. Woodland, and G. P. Brey. 2009. 'Thermal state and redox conditions of the Kaapvaal mantle: A study of xenoliths from the Finsch mine, South Africa', *Lithos*, 112: 913-23.

Li, Z. X. A., C. T. A. Lee, A. H. Peslier, A. Lenardic, and S. J. Mackwell. 2008. 'Water contents in mantle xenoliths from the Colorado Plateau and vicinity: Implications for the mantle rheology and hydration-induced thinning of continental lithosphere', *Journal of Geophysical Research-Solid Earth*, 113.

Lieberman, J. E., and J. M. Rice. 1986. 'Petrology of Marble and Peridotite in the Seiad Ultramafic Complex, Northern California, USA', *Journal of Metamorphic Geology*, 4: 179-99.

Lundquist, S. M. 1983. 'Deformation history of the ultramafic and associated metamorphic rocks of the Seiad complex, Seiad Valley, California [M.S. thesis];' *Seattle, University of Washington*: 167.

Manning, C. E. 2018. 'Fluids of the Lower Crust: Deep Is Different', *Annual Review of Earth and Planetary Sciences, Vol 46*, 46: 67-97.

Manning, C. E., and L. Y. Aranovich. 2014. 'Brines at high pressure and temperature: Thermodynamic, petrologic and geochemical effects', *Precambrian Research*, 253: 6-16.

Mattioli, G. S., and B. J. Wood. 1988. 'Magnetite Activities across the Mgal2o4-Fe3o4 Spinel Join, with Application to Thermobarometric Estimates of Upper Mantle Oxygen Fugacity', *Contributions to Mineralogy and Petrology*, 98: 148-62.

Medaris, L. G. 1966. 'Geology of The Seiad Valley Area, Siskiyou County, California, and petrology of the Seiad ultramafic complex [Ph.D. thesis]', *University of California, Los Angeles*: 395.

———. 1975. 'Coexisting Spinel and Silicates in Alpine Peridotites of Granulite Facies', *Geochimica et Cosmochimica Acta*, 39: 947-58.

Miller, M. M., and J. B. Saleeby. 1991. 'Permian and Triassic Paleogeography of the Eastern Klamath Arc and Eastern Hayfork Subduction Complex, Klamath Mountains, California - Evidence from Lithotectonic Associations and Detrital Zircon', *Aapg Bulletin-American Association of Petroleum Geologists*, 75: 375-75.

Miller, W. G. R., T. J. B. Holland, and S. A. Gibson. 2016. 'Garnet and Spinel Oxybarometers: New Internally Consistent Multi-equilibria Models with Applications to the Oxidation State of the Lithospheric Mantle', *Journal of Petrology*, 57: 1199-222.

Nell, J., and B. J. Wood. 1991. 'High-Temperature Electrical Measurements and Thermodynamic Properties of Fe3o4-Fecr2o4-Mgcr2o4-Feal2o4 Spinels', *American Mineralogist*, 76: 405-26.

Newton, R. C. 1989. 'Metamorphic Fluids in the Deep Crust', *Annual Review of Earth and Planetary Sciences*, 17: 385-412.

Newton, R. C., L. Y. Aranovich, E. C. Hansen, and B. A. Vandenheuvel. 1998. 'Hypersaline fluids in Precambrian deep-crustal metamorphism', *Precambrian Research*, 91: 41-63.

Newton, R. C., J. V. Smith, and B. F. Windley. 1980. 'Carbonic Metamorphism, Granulites and Crustal Growth', *Nature*, 288: 45-50.

Nicholls, I. A., and A. E. Ringwood. 1972. 'Production of Silica-Saturated Tholeiitic Magmas in Island Arcs', *Earth and Planetary Science Letters*, 17: 243-46.

Nicholls, L. A., and A. E. Ringwood. 1973. 'Effect of Water on Olivine Stability in Tholeiites and Production of Silica-Saturated Magmas in Island-Arc Environment', *Journal of Geology*, 81: 285-300.

Nimis, P., and H. Grutter. 2010. 'Internally consistent geothermometers for garnet peridotites and pyroxenites', *Contributions to Mineralogy and Petrology*, 159: 411-27.

Nimis, P., and W. R. Taylor. 2000. 'Single clinopyroxene thermobarometry for garnet peridotites. Part I. Calibration and testing of a Cr-in-Cpx barometer and an enstatite-in-Cpx thermometer', *Contributions to Mineralogy and Petrology*, 139: 541-54.

Novella, D., D. J. Frost, E. H. Hauri, H. Bureau, C. Raepsaet, and M. Roberge. 2014. 'The distribution of H2O between silicate melt and nominally anhydrous peridotite and the onset of hydrous melting in the deep upper mantle', *Earth and Planetary Science Letters*, 400: 1-13.

O'Neill, H. S., and V. J. Wall. 1987. 'The Olivine Ortho-Pyroxene Spinel Oxygen Geobarometer, the Nickel Precipitation Curve, and the Oxygen Fugacity of the Earths Upper Mantle', *Journal of Petrology*, 28: 1169-91.

Ohmoto, H., and D. Kerrick. 1977. 'Devolatilization Equilibria in Graphitic Systems', *American Journal of Science*, 277: 1013-44.

Peslier, A. H. 2010. 'A review of water contents of nominally anhydrous natural minerals in the mantles of Earth, Mars and the Moon', *Journal of Volcanology and Geothermal Research*, 197: 239-58.

Peslier, A. H., M. Schonbachler, H. Busemann, and S. I. Karato. 2017. 'Water in the Earth's Interior: Distribution and Origin (vol 212, pg 743, 2017)', *Space Science Reviews*, 212: 811-11.

Peslier, A. H., A. B. Woodland, D. R. Bell, and M. Lazarov. 2010. 'Olivine water contents in the continental lithosphere and the longevity of cratons', *Nature*, 467: 78-U108.

Popp, R. K., H. A. Hibbert, and W. M. Lamb. 2006. 'Oxy-amphibole equilibria in Ti-bearing calcic amphiboles: Experimental investigation and petrologic implications for mantle-derived amphiboles', *American Mineralogist*, 91: 54-66.

Popp, R. K., D. Virgo, and M. W. Phillips. 1995. 'H deficiency in kaersutitic amphiboles: Experimental verification', *American Mineralogist*, 80: 1347-50.

Powell, R. 1983. "Processes in granulite-facies metamorphism." In *Migmatites, melting and metamorphism; Proceedings/Meeting High grade metamorphism, migmatites and melting of the Geochemical Group of the Mineralogical Society of the University of Glasgow*, edited by M. P. Atherton and C. D. Gribble, 127-39. Shiva Publ., Nantwich, United Kingdom.

Powell, R., T. Holland, and B. Worley. 1998. 'Calculating phase diagrams involving solid solutions via non-linear equations, with examples using THERMOCALC', *Journal of Metamorphic Geology*, 16: 577-88.

Powers, R. E., and S. R. Bohlen. 1985. 'The Role of Synmetamorphic Igneous Rocks in the Metamorphism and Partial Melting of Metasediments, Northwest Adirondacks', *Contributions to Mineralogy and Petrology*, 90: 401-09.

Rosenthal, A., E. H. Hauri, and M. M. Hirschmann. 2015. 'Experimental determination of C, F, and H partitioning between mantle minerals and carbonated basalt, CO2/Ba and CO2/Nb systematics of partial melting, and the CO2 contents of basaltic source regions (vol 412, pg 77, 2015)', *Earth and Planetary Science Letters*, 419: 228-28.

Rudnick, R. L., L. D. Ashwal, and D. J. Henry. 1984. 'Fluid Inclusions in High-Grade Gneisses of the Kapuskasing Structural Zone, Ontario - Metamorphic Fluids and Uplift Erosion Path', *Contributions to Mineralogy and Petrology*, 87: 399-406.

Sack, R. O., and M. S. Ghiorso. 1989. 'Importance of Considerations of Mixing Properties in Establishing an Internally Consistent Thermodynamic Database - Thermochemistry of Minerals in the System Mg2sio4-Fe2sio4-Sio2', *Contributions to Mineralogy and Petrology*, 102: 41-68.

———. 1991. 'An Internally Consistent Model for the Thermodynamic Properties of Fe-Mg-Titanomagnetite-Aluminate Spinels', *Contributions to Mineralogy and Petrology*, 106: 474-505.

———. 1994. 'Thermodynamics of Multicomponent Pyroxenes .1. Formulation of a General-Model', *Contributions to Mineralogy and Petrology*, 116: 277-86.

Santosh, M. 1985. 'Fluid Evolution Characteristics and Piezothermic Array of South Indian Charnockites', *Geology*, 13: 361-63.

Santosh, M., and S. Omori. 2008a. 'CO2 windows from mantle to atmosphere: Models on ultrahigh-temperature metamorphism and speculations on the link with melting of snowball Earth', *Gondwana Research*, 14: 82-96.

———. 2008b. 'CO(2) flushing: A plate tectonic perspective', *Gondwana Research*, 13: 86-102.

Schreurs, J. 1984. 'The Amphibolite Granulite Facies Transition in West Uusimaa, Sw Finland - a Fluid Inclusion Study', *Journal of Metamorphic Geology*, 2: 327-41.

Skogby, H. 2006. 'Water in natural mantle minerals I: Pyroxenes', *Water in Nominally Anhydrous Minerals*, 62: 155-67.

Snoke, A. W., and C. G. Barnes. 2006. 'The development of tectonic concepts for the Klamath Mountains province, California and Oregon', *Geological Studies in the Klamath Mountains Province, California and Oregon*, 410: 1-29.

Spear, F. S. 1993. *Metamorphic Phase Equilibria and Pressure-Temperature Time Paths* (Mineralogical Society of America: Washington, D.C.).

Stachel, T., K. S. Viljoen, P. McDade, and J. W. Harris. 2004. 'Diamondiferous lithospheric roots along the western margin of the Kalahari Craton - the peridotitic inclusion suite in diamonds from Orapa and Jwaneng', *Contributions to Mineralogy and Petrology*, 147: 32-47.

Taylor, W. R. 1998. 'An experimental test of some geothermometer and geobarometer formulations for upper mantle peridotites with application to the thermobarometry of fertile Iherzolite and garnet websterite', *Neues Jahrbuch Fur Mineralogie-Abhandlungen*, 172: 381-408.

Touret, J., and P. Dietvorst. 1983. 'Fluid Inclusions in High-Grade Anatectic Metamorphites', *Journal of the Geological Society*, 140: 635-49.

Touret, J. L. R. 1992. 'Co2 Transfer between the Upper Mantle and the Atmosphere - Temporary-Storage in the Lower Continental-Crust', *Terra Nova*, 4: 87-98.

Touret, J. L. R., and J. M. Huizenga. 2012. 'Fluid-assisted granulite metamorphism: A continental journey', *Gondwana Research*, 21: 224-35.

Touret, Jacques. 1971. 'The granulite facies in southern Norway; 2, The fluid inclusions
Le facies granulite en Norvege meridionale; II, Les inclusions fluides', *Lithos (Oslo)*, 4: 423-36.

Valley, J. 1985. *Polymetamorphism in the Adirondacks: Wollastonite at Contacts of Shallowly Intruded Anorthosite*.

Valley, J. W. 1992. 'Granulite Formation Is Driven by Magmatic Processes in the Deep Crust', *Earth-Science Reviews*, 32: 145-46.

Valley, J. W., S. R. Bohlen, E. J. Essene, and W. Lamb. 1990. 'Metamorphism in the Adirondacks .2. The Role of Fluids', *Journal of Petrology*, 31: 555-96.

Valley, J. W., James McLelland, Eric J. Essene, and William Lamb. 1983. 'Metamorphic fluids in the deep crust; evidence from the Adirondacks', *Nature (London)*, 301: 226-28.

Walther, J. V., and P. M. Orville. 1982. 'Volatile Production and Transport in Regional Metamorphism', *Contributions to Mineralogy and Petrology*, 79: 252-57.

Warren, J. M., and E. H. Hauri. 2014. 'Pyroxenes as tracers of mantle water variations', *Journal of Geophysical Research-Solid Earth*, 119: 1851-81.

Watson, E. B., and J. M. Brenan. 1987. 'Fluids in the Lithosphere .1. Experimentally-Determined Wetting Characteristics of Co2-H2o Fluids and Their Implications for Fluid Transport, Host-Rock Physical-Properties, and Fluid Inclusion Formation', *Earth and Planetary Science Letters*, 85: 497-515.

Wood, B. J. 1990. 'An Experimental Test of the Spinel Peridotite Oxygen Barometer', *Journal of Geophysical Research-Solid Earth and Planets*, 95: 15845-51.

Wood, B. J., L. T. Bryndzia, and K. E. Johnson. 1990. 'Mantle Oxidation-State and Its Relationship to Tectonic Environment and Fluid Speciation', *Science*, 248: 337-45.

Wood, B. J., and D. Virgo. 1989. 'Upper Mantle Oxidation-State - Ferric Iron Contents of Lherzolite Spinels by Fe-57 Mossbauer-Spectroscopy and Resultant Oxygen Fugacities', *Geochimica et Cosmochimica Acta*, 53: 1277-91.

Wood, B. J., and J. V. Walther. 1983. 'Rates of Hydrothermal Reactions', *Science*, 222: 413-15.

Woodland, A. B., and M. Koch. 2003. 'Variation in oxygen fugacity with depth in the upper mantle beneath the Kaapvaal craton, Southern Africa', *Earth and Planetary Science Letters*, 214: 295-310.

Woodland, A. B., J. Kornprobst, and B. J. Wood. 1992. 'Oxygen Thermobarometry of Orogenic Lherzolite Massifs', *Journal of Petrology*, 33: 203-30.

Wright, J. E., and M. R. Fahan. 1988. 'An Expanded View of Jurassic Orogenesis in the Western United-States Cordillera - Middle Jurassic (Pre-Nevadan) Regional Metamorphism and Thrust Faulting within an Active Arc Environment, Klamath Mountains, California', *Geological Society of America Bulletin*, 100: 859-76.

Wright, J. E., and S. J. Wyld. 1994. 'The Rattlesnake Creek Terrane, Klamath Mountains, California - an Early Mesozoic Volcanic Arc and Its Basement of Tectonically Disrupted Oceanic-Crust', *Geological Society of America Bulletin*, 106: 1033-56.

Zhang, C., and Z. H. Duan. 2009. 'A model for C-O-H fluid in the Earth's mantle', *Geochimica et Cosmochimica Acta*, 73: 2089-102.

APPENDIX

Core and Rim Temperatures

Sample:	T98 core	T98 rim
WSD1	792	732
WSD2	769	764
WSD3	752	742
WSD4	802	799
WSD17	809	827

Estimated Mineral Abundances

Sample:	Olivine	Pyroxene	Spinel	Amphibole
WSD17	75%	15%	5%	5%
WSD4	75%	15%	5%	5%
WSD1	65%	20%	5%	10%
WSD2	55%	25%	5%	15%
WSD3	45%	30%	5%	20%

Olivine Compositions

Sample:	WSD1	WSD2	WSD3	WSD4	WSD17
SiO2	40.59	40.53	40.89	40.38	39.93
FeO	10.52	9.88	10.84	9.84	9.50
MnO	0.16	0.15	0.17	0.12	0.12
MgO	47.84	48.54	47.83	48.38	48.41
NiO	0.39	0.36	0.36	0.42	0.37
SUM	99.49	99.46	100.08	99.14	98.45
Mg#	0.89	0.90	0.89	0.90	0.90

Spinel Compositions

Sample:	WSD1		WSD2		WSD3		WSD4		WSD17	
	rim	core	rim	core	rim	core	rim	core	rim	core
SiO2	0.00	0.00	0.00	0.00	0.00	0.00	0.00	0.00	0.00	0.00
TiO2	0.02	0.04	0.04	0.04	0.07	0.10	0.03	0.02	0.04	0.05

Al2O3	55.71	55.27	57.34	56.82	47.33	49.26	56.17	54.17	55.15	52.99
Cr2O3	9.94	10.32	8.19	9.57	17.02	14.65	10.49	12.35	11.35	13.06
FeO	13.62	14.07	13.39	13.02	18.72	17.64	13.21	13.76	12.68	13.33
MnO	0.17	0.16	0.08	0.08	0.10	0.13	0.05	0.10	0.07	0.09
NiO	0.32	0.32	0.37	0.36	0.24	0.23	0.29	0.31	0.31	0.28
MgO	18.07	18.07	18.66	18.55	14.99	16.00	18.43	17.92	18.75	18.30
CaO	0.00	0.00	0.00	0.00	0.00	0.00	0.00	0.00	0.04	0.00
ZnO	0.18	0.22	0.19	0.15	0.35	0.30	0.21	0.21	0.12	0.13
V2O3	0.10	0.07	0.06	0.04	0.16	0.14	0.05	0.05	0.08	0.09
Sum	98.14	98.55	98.31	98.63	98.99	98.44	98.93	98.89	98.60	98.32
Fe2O3	0.95	1.46	1.40	0.61	2.39	2.88	0.56	0.74	0.93	1.31
FeO	12.77	12.76	12.14	12.47	16.57	15.05	12.70	13.10	11.85	12.16
Sum	98.23	98.69	98.45	98.69	99.23	98.73	98.99	98.96	98.69	98.45
FeIII/II+III	0.06	0.09	0.09	0.07	0.11	0.15	0.10	0.05	0.07	0.09
Mg#	0.73	0.73	0.74	0.74	0.63	0.66	0.73	0.72	0.75	0.74

Amphibole Compositions

Sample:	WSD1	WSD2	WSD3	WSD4	WSD17
SiO2	43.12	42.89	45.45	43.55	43.71
Al2O3	14.74	14.94	12.79	14.90	14.23
TiO2	1.28	1.13	0.78	0.78	1.36
Cr2O3	0.83	1.00	0.84	0.74	0.89
FeO	3.57	3.40	3.94	3.56	3.66
MnO	0.03	0.04	0.05	0.04	0.04
MgO	17.63	17.68	18.57	18.10	18.04
CaO	12.00	12.30	12.38	12.21	12.40
NiO	0.09	0.09	0.08	0.10	0.10
Na2O	2.87	3.02	1.73	2.66	2.66
K2O	0.05	0.11	0.11	0.18	0.00
F	0.05	0.03	0.05	0.04	0.04
SUM	96.19	96.60	96.72	96.83	97.08
O=F	0.02	0.01	0.02	0.01	0.02
SUM	96.17	96.59	96.69	96.82	97.06
H2O	1.87	1.91	1.72	1.83	1.84
SUM	98.04	98.49	98.42	98.65	98.90

Orthopyroxene Compositions

Sample:	WSD1		WSD2		WSD3		WSD4		WSD17	
	rim	core	rim	core	rim	core	rim	core	rim	core
SiO2	57.18	55.88	56.06	55.57	55.69	56.13	56.44	56.20	55.42	55.43
TiO2	0.06	0.06	0.06	0.06	0.10	0.07	0.04	0.04	0.10	0.06
Al2O3	1.81	2.76	2.43	2.98	2.09	2.35	2.70	3.05	2.89	3.16
Cr2O3	0.09	0.17	0.12	0.21	0.15	0.15	0.25	0.21	0.22	0.22
FeO	7.02	6.88	6.68	6.71	7.51	7.34	6.57	6.45	6.44	6.33
MnO	0.18	0.17	0.17	0.15	0.21	0.17	0.19	0.16	0.16	0.13
NiO	0.07	0.07	0.08	0.08	0.07	0.08	0.07	0.07	0.06	0.05
MgO	34.47	33.84	34.09	34.15	32.98	33.66	34.29	33.95	33.99	33.88
CaO	0.29	0.41	0.33	0.42	0.32	0.38	0.36	0.46	0.42	0.44
Sum	101.18	100.24	100.02	100.33	99.10	100.34	100.89	100.59	99.70	99.70
	0.00	0.00	0.00	0.00	0.00	0.00	0.00	0.00	0.00	0.00
Fe2O3	0.72	1.20	1.15	2.05	0.34	1.00	0.97	0.61	1.58	1.25
FeO	6.37	5.80	5.64	4.87	7.21	6.44	5.69	5.90	5.02	5.20
Sum	101.25	100.36	100.13	100.54	99.14	100.44	100.99	100.65	99.86	99.83
FeIII/II+III	0.09	0.16	0.16	0.27	0.04	0.12	0.13	0.08	0.22	0.18
Mg#	0.91	0.91	0.92	0.93	0.89	0.90	0.91	0.91	0.92	0.92

Clinopyroxene Compositions

Sample:	WSD1		WSD2		WSD3		WSD4		WSD17	
	rim	core	rim	core	rim	core	rim	core	rim	core
SiO2	53.06	52.49	53.50	52.75	52.98	52.84	53.11	53.07	51.98	51.85
TiO2	0.30	0.30	0.14	0.25	0.19	0.17	0.19	0.17	0.34	0.36
Al2O3	3.00	3.43	2.13	3.65	1.87	2.12	2.79	3.31	3.79	4.03
Cr2O3	0.30	0.34	0.18	0.37	0.20	0.21	0.30	0.42	0.37	0.48
FeO	2.40	2.42	2.20	2.18	2.33	2.45	2.24	2.40	2.42	2.33
MnO	0.07	0.10	0.08	0.10	0.08	0.08	0.09	0.08	0.10	0.11
NiO	0.04	0.06	0.06	0.03	0.03	0.02	0.04	0.04	0.05	0.04
MgO	16.93	16.65	17.40	16.64	17.17	17.02	17.26	17.05	16.84	16.72
CaO	23.50	23.37	23.93	23.61	24.05	24.20	23.78	23.72	23.29	23.54
Na2O	0.27	0.30	0.27	0.38	0.09	0.10	0.22	0.27	0.26	0.28
K2O	0.00	0.00	0.00	0.00	0.00	0.00	0.00	0.00	0.00	0.00
Sum	99.88	99.45	99.90	99.96	98.99	99.19	100.01	100.51	99.43	99.74
Fe2O3	0.35	0.61	1.31	0.75	0.84	1.10	1.04	1.05	1.29	1.59
FeO	2.09	1.87	1.02	1.51	1.58	1.46	1.30	1.45	1.26	0.90
Sum	99.92	99.51	100.03	100.03	99.08	99.30	100.12	100.62	99.56	99.90
FeIII/II+III	0.13	0.22	0.54	0.31	0.32	0.40	0.42	0.39	0.48	0.62
Mg#	0.94	0.94	0.97	0.95	0.95	0.95	0.96	0.95	0.96	0.97